NON-MAXWELLIAN VELOCITY DISTRIBUTION FUNCTIONS

ASSOCIATED WITH STEEP TEMPERATURE

GRADIENTS IN THE SOLAR TRANSITION REGION

Paper I. Estimate of the Electron Velocity

Distribution Functions

Robert Roussel-Dupré[*]

Department of Astro-Geophysics
University of Colorado
Boulder, Colo.   80309, U.S.A.

*Presently at University of Hawaii, Institute for Astronomy, 2680 Woodlawn
Drive, Honolulu, Hawaii 96822, U.S.A.

ABSTRACT

We show that, in the presence of the steep temperature gradients characteristic of EUV models of the solar transition region, the electron and proton velocity distribution functions are non-Maxwellian and are characterized by high energy tails. We estimate the magnitude of these tails for a model of the transition region and compute the heat flux to be a maximum of 30% greater than predicted by collision-dominated theory.

1. INTRODUCTION

Existing models of the solar transition region, derived from observations of the solar spectrum in the extreme ultraviolet (EUV), make use of the assumption that the electron velocity distribution functions are nearly Maxwellian to compute excitation, ionization, and recombination rates. However, these models are characterized by steep temperature gradients which, as we shall show, lead to distribution functions for electrons and protons which are non-Maxwellian in contradiction with the initial assumption.

Departures from the Maxwellian distribution can be substantial (depending on the steepness of the temperature gradient) and take the form of high energy tails for those particles which are propagating down the temperature gradient. This leads to heat fluxes differing from those computed from collision-dominated theory and ionization, excitation and recombination rates differing from those computed assuming Maxwellian distribution functions for the electrons.

In this paper, we discuss the kinetic effects which give rise to high energy tails in the presence of steep gradients and estimate the magnitude of these effects for Dupree's (1972) EUV model of the transition region. We then compute various moments of the electron distribution functions and compare these to results obtained from collision dominated theory. A subsequent paper will compare the ionization equilibrium populations for ions of carbon, nitrogen, and oxygen, computed with the non-Maxwellian distribution functions obtained in this paper to those computed with the usual assumption of a Maxwellian distribution function for the electrons.

2. NON-MAXWELLIAN ELECTRON AND PROTON DISTRIBUTION FUNCTIONS

A.   Departures from Maxwellian

The collision dominated kinetic theory of non-uniform gases was developed by Chapman and Enskog in the 1920's and is expounded by Chapman and Cowling in "The Mathematical Theory of Non-Uniform Gases" (1970). The Chapman-Enskog theory assumes that the distribution function for a given species, α, can be written in general as,

$$f_\alpha(\underline{x},\underline{v},t) = f_\alpha^{(0)}(\underline{x},\underline{v},t) + f_\alpha^{(1)}(\underline{x},\underline{v},t) + f_\alpha^{(2)}(\underline{x},\underline{v},t) + \ldots \qquad (1)$$

where each of the $f_\alpha^{(n)}$ represents a successive approximation to the total distribution function and each satisfies the condition,

$$\left| \frac{f_\alpha^{(n)}}{f_\alpha^{(n-1)}} \right| \ll 1, \text{ for all } \underline{x}, \underline{v},$$ and t. The full Boltzmann equation

is then solved with what amounts to a perturbation scheme. The zeroth order solution, $f_\alpha^{(0)}$, is a Maxwellian distribution function characterized by a temperature, T, density, n, and mean flow, $\underline{v}_0$.

Spitzer and Härm (1953) computed the first order electron distribution function, $f_e^{(1)}$, in the presence of a temperature gradient for a gas of mean ionic charge Z defined by,

$$Z \equiv \sum_i n_i Z_i^2 / n_e \qquad (2)$$

with the sum taken over all positive ions. In Spitzer and Härm's notation, the total electron distribution function, to first order, is given by,

$$f_e = f_e^{(0)}\left(1 + \mu D_e(u,z)\right). \tag{3}$$

where u is the electron speed normalized to the thermal speed and μ is the cosine of the polar angle in velocity space.

In Table II of Spitzer and Härm the quantity $\bar{Z} D_e(u,z)/B_e$ is tabulated as a function of u, where $B_e \left(= \dfrac{2k^2 T_e |\nabla T_e|}{\pi n_e e^4 \ell n \Lambda}\right)$ is the ratio of the electron mean free path to temperature scale length and Λ is the number of particles in a Debye sphere. We note that $D_e(u,z)/B_e$ is a function of u only and that this quantity increases rapidly with u. In Figure 1, we plot B_e as a function of log T_e for Dupree's transition-region model.

Since departures from Maxwellian are large when $|\mu D_e(u,z)| \geq 1$, we define a critical energy (u_c^2) such that $|D_e(u_c,z)| \simeq 1$. In Figure 2 we plot u_c^2 as a function of log T throughout the transition region for Dupree's model. We find that, where the temperature gradient is steepest (T $\sim 10^{5.2}$ K), substantial deviations from Maxwellian exist at energies greater than or equal to approximately 6 kT. We will show that this result has important implications for ionization equilibrium and heat flux calculations.

A similar analysis can be carried out for the protons given the first order distribution function computed by Roussel-Dupré (1979). In Figure 3, we plot the critical energy (u_c) at which $|D_i(u_c,z)| = 1$ as a function of proton temperature, assumed to equal the electron temperature. We find that, where the temperature gradient is steepest (T $\sim 10^{5.2}$ K), substantial deviations from Maxwellian exist again at energies greater than or approximately equal to 6 kT. We now ask in what way we may expect these distribution functions to differ from a Maxwellian.

B. High Energy Tail

Consider a plane-parallel layer of gas, with z as the vertical coordinate, composed of field particles having a Maxwellian distribution locally with temperature, T_f, and density, n_f, each varying as a function of z according to Dupree's model for the transition region. We now inject test particles with velocity, $\underline{v}$, parallel to the z-direction and determine the rate at which the test particle's velocity and kinetic energy change as a result of encounters with field particles. From these rates, we then obtain the time, t_D, for a test particle to undergo a 90° deflection and the time, t_E, for a test particle to thermalize to the local field particle temperature.   This problem was worked out by Spitzer (1962), cf., his page 132.

Given that the field particles have a non-uniform temperature in the z-direction, we can define another time scale; namely, the time it takes for a test particle with velocity, $\underline{v}$, to travel a temperature scale length. We have,

$$t_F = \frac{1}{v|\mu|}\left(\frac{1}{T_f}\frac{dT_f}{dz}\right)^{-1} . \tag{4}$$

Examination of the energy dependence of the ratios t_D/t_F and t_E/t_F reveals that both ratios increase rapidly with test particle energy. It is possible then to define critical test particle energies, $(u_c^2)_D$ and $(u_c^2)_E$, above which t_D/t_F and t_E/t_F, respectively, become greater than one. In Figure 4, the solid and dashed curves represent plots of $(u_c^2)_D$ and $(u_c^2)_E$, as a function of Log T through the transition region with electrons as the test particles. We find that, where the temperature gradient is steepest, the deflection time becomes on the same order as a

time of flight (t_F) for energies greater than or approximately equal to 10 kT. Since test electrons with energies greater than $(u_c{}^2)_D$ can penetrate a temperature-scale length without undergoing a 90° deflection, high energy electrons from the corona can penetrate quite far into the transition region while the colder test electrons from the chromosphere will not penetrate as far. This leads to an anisotropic velocity distribution function.

Similarly, we find that $t_E/t_F \geq 1$ for energies ≥ 5 kT at $T = 10^{5.2}$ and since test electrons with energy greater than $(u_c{}^2)_E$ will maintain their energy over scales greater than a temperature scale length, high energy electrons from the corona will populate the high energy tail of the field electron distribution function. Thus, the final self-consistent distribution functions will possess high energy tails which are highly anisotropic.

The values of $(u_c{}^2)_D$ and $(u_c{}^2)_E$ for proton test particles are plotted as functions of log T in Figure 5. The protons clearly will also form non-Maxwellian distribution functions, just as the electrons. An interesting difference, however, stems from the fact that for the most part electrons and protons do not exchange energy. A proton test particle may thermalize to a temperature which is completely different from the electron temperature. This follows since t_E (p-e collisions) $\sim \left(\frac{m_p}{m_e}\right)^{\frac{1}{2}} t_E$ (p-p collisions).

The ions responsible for the EUV line emission present a different scenario. Since the ion abundances relative to the protons and electrons are quite small, and since their masses are much larger than the electron mass, they will interact primarily with protons. Furthermore, the average charge of ions formed from 10^5K to 10^6K ranges from $Z = 3$ to $Z = 10$ and since t_D and t_E are both inversely proportional to Z^2, the ions

will usually isotropize to nearly Maxwellian distribution functions and thermalize to the proton temperature. To illustrate this result, we have carried out an analysis on Si IV similar to that carried out for the electrons. In Figure 6, we plot $(u_c^2)_D$ and $(u_c^2)_E$ vs. Log T, for Si IV and find that these critical energies are much larger than for the electrons and protons. Thus the ion distribution functions are nearly Maxwellian. An interesting consequence of these results is that EUV line profiles will reflect the proton temperature but not necessarily the electron temperature and will not reflect any asymmetries which might arise in either the electron or proton distribution function. We note, however, that the latter conclusion applies only to the extent that we have neglected the first order correction (to the zeroth order Maxwellian distribution function) obtained from collision-dominated theory. Indeed, thermal diffusion (a process which is manifested in the first order ion distribution functions [cf., Roussel-Dupré,1979]) of the heavy ions clearly reflects the asymmetries associated with the first order electron and proton distribution functions.

As a final note we emphasize that, while it is true that there will always exist particles with high enough energy to be collisionless in the transition region, the supply of such particles is limited by the ultimate source of energy, i.e., the solar corona. Thus, let us assume that the coronal electron distribution function is a Maxwellian with temperature 10^6K, the fraction f of particles with energy greater than u^2 is listed in Table I. We find that at T = 10^5K, for example, 76 percent of coronal electrons have energy greater than 6 kT; however, only two percent have energy greater than 50 kT. The point is that the critical energies at which electrons become collisionless are sufficiently

low through the upper half of the transition region that a substantial number of coronal electrons are collisionless through that region. As a result, large departures from Maxwellian can be expected in the region from 10^5 to 10^6K.

3. PARTICLE ORBITS

In the previous section, we showed that high speed test electrons, moving along the temperature gradient in the transition region, could penetrate a temperature scale length without undergoing a 90° deflection or losing a significant fraction of their initial energies. The analysis which brought us to these conclusions, however, was based only on a rather simple minded comparison of appropriate time scales. In this section, we shall develop these ideas on a more quantitative basis.

We shall first discuss some properties of the 'dynamical-friction' force exerted on a test electron as it moves through a fully ionized. gas. This force is taken from the Fokker-Planck collision operator (cf., Dreicer, 1959) and is given for a test electron of velocity $\underline{v}$ by the expression

$$\underline{F}_D = m_e \Gamma_e \frac{\partial}{\partial \underline{v}} \sum_f z_f^2 \left(\frac{m_f + m_e}{m_f} \right) \int \frac{f_f(\underline{v}')\,d\underline{v}'}{|\underline{v} - \underline{v}'|} \qquad (5)$$

where $\Gamma_e = \dfrac{4\pi e^4 \ell n \Lambda}{m_e^2}$,

$f_f(\underline{v})$ is the field particle velocity distribution function, the sum is over all field particles, and the integral over all velocity space. For the special case where the field particles have Maxwellian distribution functions and consist of electrons and protons, equation (5) reduces to,

$$\underline{F}_D = \frac{-e\, E_c}{u^2} \left(2\Lambda(u) + \Lambda(\beta_p u) \right) \frac{\underline{v}}{v} \qquad (6)$$

where $\quad E_c = n\, {}^m e/e\; \Gamma_e a_e,\; \beta_p = \left(\frac{m_p}{m_e}\right)^{\frac{1}{2}}$

$$a_e = \left(\frac{m_e}{2kT}\right),$$

$$\Lambda(u) = \phi(u) - u\phi'(u) ,$$

$$\phi(u) = \frac{2}{\sqrt{\pi}} \int_0^u \exp(-t^2)dt ,$$

and n and T are the field particle density and temperature respectively. In Table II we list the absolute value of $\underline{F}_D$, normalized to eE_c, as a function of u. We see that the dynamical friction increases sharply up to the proton thermal speed ($\beta_p u = 1$) and then decreases for larger u. For high speed test particles (i.e., u >> 1) $|\underline{F}_D|$ decreases as $1/u^2$ while for those moving at very low speeds (i.e., $\beta_p u << 1$) $|F_D|$ becomes proportional to u. This behavior of the dynamical friction force is responsible for runaway effects associated with high speed particles and the drifting of thermal particles in a plasma subject to an externally applied field. For a gas with a temperature gradient, we will find that we can describe velocity space in terms of a collision-dominated part populated by particles which are cooled by dynamical friction as they move from higher temperatures to lower temperatures; and a collisionless regime populated by high speed test particles which can penetrate down through a temperature scale length without cooling substantially. An electric field applied along the temperature gradient will have the effect of accelerating electrons into the collisionless regime, leading to an increase in the population of the high energy tail. We will illustrate these effects more clearly by computing the orbits of high

speed electrons in velocity space, with an analysis similar to that used by Dreicer (1960).

Consider a single test electron with velocity $\underline{v}$ moving through a plane-parallel layer composed of electrons and protons whose distribution functions are Maxwellian and described by a density, n, and temperature, T. For generality we include the effects of an externally applied electric field and allow the temperature of the field particles to vary along the vertical coordinate, z, of the layer but, for simplicity, we assume that the temperature gradient and density remain constant. Under these conditions, the Langevin equation for the change in velocity $\underline{v}$ is, cf., Chandrasekhar (1943) for details,

$$\frac{d\underline{v}}{dt} + \frac{3eE_c}{m_e a_e} \frac{\underline{v}}{v^3} = \frac{-e\underline{E}}{m_e} + \underline{A}(t) \quad . \tag{7}$$

In this equation, the acceleration due to particle-particle interactions is separated into a time-averaged part, the dynamical friction, and a part, $\underline{A}(t)$, describing fluctuations about the average. The second term on the left hand side of equation (7) is simply the high velocity limit of the dynamical friction. The parameter, t, represents the time as we follow the test electron along its trajectory through the gas, and is related to the coordinate, z, by the equation,

$$\frac{dz}{dt} = v_z \tag{8}$$

Ignoring the velocity fluctuations produced by the acceleration $\underline{A}(t)$ (See Dreicer, 1960) and combining equations (7) and (8) we can write the Langevin equation as,

$$\mu V \frac{dT}{dz} \frac{dv}{dT} + \frac{3eE_c}{a_e m_e} \frac{v}{v^3} = \frac{-eE}{m_e} \qquad (9)$$

We can reduce equation (9) into two component equations which in non-dimensional form are,

$$\mu \frac{dx^2}{d\theta} = - \frac{\delta}{u_b^2} \left(\frac{1}{x^2} + \mu \right) \qquad (10)$$

$$\mu \frac{d\mu}{d\theta} = - \frac{\delta}{2u_b^2} \frac{(1 - \mu^2)}{x^2} \qquad (11)$$

where

$$x^2 = u^2/u_b^2 \quad, \quad u_b^2 = 3E_{c/E}^0 \quad,$$

$$\theta = T/T_0 \quad, \quad \delta = \frac{eEL}{kT_0} \quad, \quad L = \left(\frac{1}{T_0} \frac{dT_0}{dz} \right)^{-1} \quad,$$

and a subscript zero indicates that the parameter is to be evaluated at the initial position of the test electron. The flow lines for fast electrons in velocity space in any plane containing E, are obtained from equations (10) and (11),

$$\frac{dx^2}{d\mu} = \frac{2}{(1-\mu^2)} \left(1 + \mu x^2 \right) \qquad (12)$$

The solution to this equation is,

$$x^2 = \frac{-2}{1+\mu} + \frac{K}{1-\mu^2} \qquad (13)$$

where $K = ((1+\mu_0)x_0^2 + 2)(1 - \mu_0)$,

and x_0 and μ_0 are the values of x and μ at the initial position of the

test electron. Note that equation (13) generates essentially the same flow lines obtained by Dreicer.

The dynamical friction acts to accelerate test particles in a direction which always opposes their motion. This arises simply from the fact that the field particles are distributed symmetrically in velocity space. For the special case $E = 0$ the flow lines are generated by the equation $\mu =$ constant so that, in velocity space, the test particles simply follow straight line orbits leading into the origin. The relevant problem for a test particle moving through a finite layer is to find its final velocity after it leaves the layer, given its initial velocity $\underline{u}_0$. By computing the work done by the dynamical friction on a test electron as it moves through the layer and given its initial velocity, we can derive its final velocity after it leaves the layer. As shown in Appendix 1, this is given in general by the equation,

$$u_f^4 = u_0^4 \left(1 - \frac{2\delta_c}{u_0^4} \frac{\theta_f - \theta_0}{\mu} \right) \tag{14}$$

where u_f and u_0 are the final and initial speeds normalized to the thermal speed at the top of the layer; $\delta_c \equiv \left(\dfrac{eE_c^0 L}{kT_0} \right)$ is the work done (normalized to kT_0) by the dynamical friction on a thermal electron (at T_0), which travels a temperature scale length (L) along the temperature gradient; θ_0 and θ_f are the initial and final temperatures normalized to T_0. Equation (14) neglects the effect of deflections in slowing a beam of test particles.

In Figure 7, we plot, on a v_z vs. v_x graph the final velocities for test electrons injected into a given layer in the transition region (characterized by its critical speed, u_c, computed from Dupree's model)

for two initial energies, $u_0^2 = 1.5u_c^2$ and $u_0^2 = 2.0u_c^2$.[*] The circle in

---

[*]The critical speed (u_c) referred to here is that for a 90° deflection
$(= (u_c)_D)$.

---

this plot represents the distribution of initial velocities, all with

the same magnitude, for test electrons injected at different angles to

the temperature gradient. Note that those particles with positive

initial μ-values are injected at the bottom of the layer; while those

with negative μ-values are injected at the top. The straight lines are

the particle flow lines which are drawn in to simplify the tracing of

the particle trajectory from its initial velocity to its final velocity

after it leaves the layer. Clearly, particles injected at large angles

(small μ) to the temperature gradient never make it out of the layer.

These test electrons simply come to rest somewhere in the layer itself.[*]

---

[*]We note that a single test particle can never actually come to rest

because of the effect of the velocity fluctuations, A(t), which we ignored

in this analysis. Furthermore, remember that our analysis only applies as

long as the test particle speed is larger than the local thermal speed.

On the other hand, those electrons moving along the temperature gradient

have small changes in their initial speeds. Another interesting effect

is associated with the μ dependence of the final speeds. We see that

the relative change in particle energies does not vary substantially

with μ until a critical value is reached, beyond which the test particle

decelerates rapidly. For higher initial energies, this critical μ-value

decreases. Thus, even if a test particle undergoes fluctuations in velocity space about its mean orbit, it does not slow substantially until it reaches large angles to the temperature gradient.

The effect of the statistical fluctuations in velocity, $\underline{A}(t)$, which was not included in this analysis, is to smear out the particle orbits in velocity space. In other words, a single test electron can jump from one flow line to another in the course of its motion through a given layer. The degree to which a particle is deflected to and from various orbits depends on its speed. The larger the particle speed, the smaller the fluctuations. Clearly, those electrons moving along the temperature gradient have the greatest chance of escaping a given layer without a substantial change in their initial speeds or directions. Those traveling at large angles to the temperature gradient, will slow because of their longer path lengths and will also deflect more easily to different flow lines. Some will be deflected into a flow line directed along the temperature gradient; however, if their speeds have decreased substantially by this time, they can be easily deflected back out again before escaping the layer. These particles become trapped in the thermal pool. Thus, the dynamical friction and $\underline{A}(t)$ combine to thermalize and isotropize the distribution of test particles to the field particle distribution. However, they become ineffective for particles at high speeds and traveling at small angles with respect to the temperature gradient. This is what leads to anisotropies and a high energy tail in velocity space for a plasma with a temperature gradient. We can conclude that velocity space can be broken up into a thermal part and a collisionless part populated by high energy electrons which stream through a temperature scale length without altering their energies substantially.

A similar analysis can be carried out for the case where an electric field is applied along the temperature gradient. Combining equations (11) and (13), we obtain a transcendental equation for the final μ-value of the test electron; namely.

$$\frac{K}{1-\mu^2} - \frac{2}{1+\mu} - \ell n \left(\frac{1+\mu}{1-\mu} \cdot \frac{1-\mu_0}{1+\mu_0} \right) = $$
$$x_0^2 \left(1 + \frac{\delta}{u_b^2 x_0^2} \quad (\theta_0 - \theta_f) \right) \tag{15}$$

From this equation and the particle trajectories (equation 13), we obtain the final test particle velocities. Equation (15) was solved numerically with an iteration scheme. Our results are displayed in Figures 8-11 with a format similar to that used for zero electric field. In this case, however, the results depend on both the value of the critical speed, u_c, for a given layer in the transition region and on $\beta = E/E_c$. In Figure 8, the final velocities are associated with initial energies of $u_0^2 = 1.5 u_c^2$ and $u_0^2 = 2.0 u_c^2$ where u_c^2 is the minimum value of $(u_c^2)_D$ plotted in Figure 4 and β was taken to be 0.5. In Figure 9, the initial velocities are the same as in Figure 8, however, the value of β was changed to 1.0. We see that the larger the initial velocities the smaller the final relative change in velocities. In addition, if the electric field is increased the relative change in velocities increases. In Figures 10-11, we plot the final velocities for a value of u_c^2 equal to twice the minimum value of $(u_c^2)_D$ for the transition region and for the same values of β. Comparing these two sets of figures, we find that the acceleration due to the electric field increases relative to that due to the dynamical friction as we move to higher speeds. This arises

from the fact that the dynamical friction force falls off as $1/u^2$ while the electric field is independent of velocity.

The most interesting features of these plots are the particle orbits. As pointed out by Dreicer (1960), there exists a critical surface which separates velocity space into a region where dynamical friction dominates and a part where the electric field dominates. The minimum distance of this surface from the origin occurs at $\mu = -1$ and is given as $u = u_b$ where $u_b^2 = 3E_c/E$. The larger the electric field, the smaller the particle speed needed for the electric field to dominate over dynamical friction. Thus the region in velocity space which is effectively collisionless becomes larger with increasing E. We also observe that this critical speed increases as μ decreases. What is more important, however, is the behavior of the final velocities as a function of μ. We find that the relative change in velocities remains approximately constant up to a critical angle, below which a test particle experiences larger changes in velocity. Indeed, the latter region is quite narrow in μ and becomes narrower the larger the initial speed of the test particles.

Finally, the effect of an electric field is essentially to accelerate test particles into the collisionless regime. If the electric field points along the temperature gradient, then the asymmetry produced by the temperature gradient is enhanced i.e., the number of high energy electrons moving down the temperature gradient is increased. The opposite applies if the electric field points in a direction opposite to the temperature gradient. Furthermore, the electric field introduces a critical surface within which a particle's motion is dominated by dynamical friction while outside of which the motion is dominated by the electric field.

4. ESTIMATE OF THE ELECTRON DISTRIBUTION FUNCTION

We have shown that the electron distribution function for velocities parallel or anti-parallel to a temperature gradient could be divided into a collision-dominated regime and a collisionless regime. If the collision dominated part of the distribution function can be represented by a Maxwellian, then for all v_x, v_y, and for a steady state with a temperature gradient in the z-direction,

$$f_e(v_x, v_y, v_z, z) = n_0 \left(\frac{m_e}{2\pi k T_0} \right)^{3/2} \exp\left[-\frac{m_e}{2kT_0} (v_x^2 + v_y^2 + v_z^2) \right] \quad (16)$$

for $v_z \geq -v_{zc}$ while for $v_z \leq v_{zc}$

$$f_e(v_x, v_y, v_z, z) = \frac{m_e}{2\pi k T_0} \exp\left[-\frac{m_e}{2kT_0} (v_x^2 + v_y^2) \right] f_{tail}(v_z, z)$$

where v_{zc} is the 'critical' speed beyond which the electrons become collisionless. We note from equation (16) that the tail is attached only at negative z-velocities. This stems from the argument that there are very few collisionless test particles originating from the lower temperatures and very few high energy particles, from high temperatures, deflected back up the temperature gradient.

Our objective, then, is to estimate the velocity dependence of the tail (f_{tail} [v_z,z]) of the electron distribution function throughout the transition region, given the density and temperature profiles from Dupree's model. We note first that the tail at a temperature, T, must ultimately originate from the underlined thermal part of distribution functions at higher temperatures.[*] As a result, the contribution to the tail at

---

[*] This conclusion stems primarily from the fact that the corona is isothermal and that the tail is populated by collisionless electrons which stream to lower energies without changing their initial energies.

temperature, T, and velocity, v_z, from the distribution function at $T + \Delta T$ and velocity v_z is given by,

$$f_{tail}(v_z, T) = n(T+\Delta T) \left(\frac{m_e}{2\pi k(T+\Delta T)} \right)^{\frac{1}{2}}$$

$$exp \left[-\frac{m_e v_z^2}{2\pi k(T+\Delta T)} \right] - v_{zc}(T+\Delta T) \leq v_z \leq -v_{zc}(T) \qquad (17)$$

where the upper limit on v_z arises from the fact that particles with larger velocities are collision dominated (not part of the tail) and the lower limit is a result of the fact that particles at lower velocities are also collisionless at $T + \Delta T$ and therefore originated ultimately from the thermal part of the distribution functions with temperatures greater than $T + \Delta T$. If we take the limit of equation (17) as ΔT approaches zero, we see that each temperature, T, contributes, at a single velocity $v_z = v_{zc}(T)$, an amount given by a Maxwellian evaluated at v_z, to the tail at lower temperatures. Therefore, the tail at temperature, T, is given in general by,

$$f_{tail}(v_z, T) = n(T') \left(\frac{m_e}{2\pi kT'} \right)^{\frac{1}{2}} exp \left[-\frac{m v_z^2}{2kT'} \right] \qquad (18)$$

for $v_z \leq -v_{zc}(T)$ and where T' is a function of v_z, derived from the equation,

$$v_{zc}(T') = v_z . \qquad (19)$$

The form for the tail is complete, given the critical speed as a function of temperature. In Section 2, we estimated the critical energies beyond which electrons become collisionless from ratios of appropriate

time scales and from collision-dominated theory. Three sets of critical energies were obtained, $(u_c^2)_D$ (90° deflection), $(u_c^2)_E$ (thermalization) and u_c^2 (collision-dominated theory). Since the latter is based on a precise mathematical solution of the Boltzmann equation, we feel that u_c^2 gives a good indication for the location of the tail in velocity space. However, u_c^2 was also derived assuming that the first order distribution function $f^{(1)}$ was equal in magnitude to $f^{(0)}$. Since strong departures from Maxwellian will occur even if $f^{(1)}$ is one-tenth of $f^{(0)}$, the critical energy should be chosen to be less than u_c^2. We have chosen to work with $(u_c^2)_E$ which is always less than u_c^2 throughout the transition region. This choice is somewhat arbitrary and should be considered a lower limit on the critical energy since electrons with energy less than $(u_c^2)_E$ are thermalized. We will also present results for a critical energy equal to $(0.4)^{\frac{1}{2}}(u_c^2)_D$. This particular choice arises in connection with the calculations of particle orbits presented in Section 3 (see also Roussel-Dupré, 1979, p. 97) and should be considered an upper limit to the critical energy.

Given the results of Section 2 for the critical energies $(u_c^2)_F$, we have

$$u_{zc}^2 = 3.28 \times 10^2 \left(\frac{n \ell n \Lambda}{T'} \left(\frac{dT'}{dz} \right)^{-1} \right)^{1/3} \qquad (20)$$

Combining equations (18), (19), and (20) and assuming that the gas pressure and the quantity $q' = T'^{5/2} dT'/dh$ are constant, we obtain

$$f_{tail}(u_z, T_0) = n_0 \left(\frac{m_e}{2\pi k T_0} \right)^{\frac{1}{2}} \left(\frac{u_{zc}^2}{u_z^2} \right)^{9/7}$$

$$\times \exp \left[- u_z^{2/7} u_{zc}^{12/7} \right] \qquad (21)$$

for $u_z \leq -u_{zc}$.

Equation (21) gives the final form for the tail of the distribution function through the transition region. In Figure 12, we plot the ratio of $f_{tail}(u_z,T_o)$ to a Maxwellian evaluated at u_z, as a function of u_z^2/u_{zc}^2 for several values of u_{zc}^2. We find that this ratio increases rapidly with velocity i.e., the tail is overpopulated compared to a Maxwellian.

Finally, implicit to the derivation of the velocity dependence of the tail was the assumption that the collisionless particles gain or lose only a small fraction of their initial energy over the extent of the transition region as a result of work done on them by external forces such as gravity. This is an excellent approximation since the transition region is so thin and since these collisionless particles have very high energies. In addition, the assumption that q' is constant is also a very good approximation for the transition region since most, if not all of the collisionless particles originate from the region $T = 10^{5.2} - 10^{6.2}$ K where $T^{5/2}$ dT/dh is indeed a constant.

5. MOMENTS OF THE ELECTRON DISTRIBUTION FUNCTION

In deriving equation (18) we assumed that the thermal part of the distribution function could be approximated by a Maxwellian. In fact, the actual distribution function is the sum of a Maxwellian plus small correction terms which result from   nonuniformities in the density, temperature and mean flow of the gas. If the correction terms are small they may be computed from a perturbation analysis - the Chapman-Enskog theory. We found in Section 2 that the first order correction term computed by Spitzer and Härm (1953) for electrons in a nonuniform gas, is small for electron energies less than a critical energy, u_c^2, plotted as a function of temperature in the transition region in Figure 2. Since the correction

term is small compared to a Maxwellian for speeds defined to be in the thermal part of the distribution function, we were justified in our approximation of the previous section. However, we cannot completely ignore the contribution of the first order term to the overall distribution function since its nonuniform nature in velocity space contributes to the moments which determine the mean gas flow and heat flux at a given height in the transition region. Since perturbation theory breaks down beyond the critical speed, u_c, this correction term can only apply to the collision dominated part of the distribution function and, therefore, does not affect the tail. In fact, the tail was computed because collision dominated theory broke down at high velocities. The total electron distribution function for all v_x and v_y becomes,

$$f_e(v_x, v_y, v_z, z) = f_e^{(0)}(v_x, v_y, v_z, z) + f_e^{(1)}(v_x, v_y, v_z, z)$$

for $v_z \geq -v_{zc}$ and   (22)

$$f_e(v_x, v_y, v_z, z) = f_e^{(0)}(v_x, v_y, z) \, f_{tail}(v_z, z)$$

for $v_z \leq -v_{zc}$ where $f_e^{(0)}$ is a Maxwellian; $f_e^{(1)}$ is taken from Spitzer and Härm (1953) and f_{tail} is given by equation (21).

The electron density, mean flow temperature, and heat flux in the transition region are defined in terms of the electron distribution function as:

Density: $n_e(z) = \int d\underline{v} \, f_e(\underline{v}, z)$

Mean Flow: $\bar{\underline{v}}_e(z) = \int d\underline{v} \, \underline{v} \, f_e(\underline{v}, z)$

Temperature: $T(z) = \dfrac{m_e}{3k} \int d\underline{v} \, (\underline{v} - \bar{\underline{v}}_e)^2 \, f_e(\underline{v}, z)$

Heat Flux: $q_e(z) = \dfrac{1}{2} m_e \int d\underline{v} \, (\underline{v} - \bar{\underline{v}}_e)^2 \, \underline{v} \, f_e(v, z)$

From equation (19), we then find,

$$n_e(z) = n_0 \left[{}^1\!/_2(1 + \phi(u_c)) + \frac{7u_c^{12}}{\sqrt{\pi}} \int_{u_c}^{\infty} \frac{\exp(-t^2)}{t^{12}} \, dt \right] \qquad (23)$$

$$\bar{u}_{ze}(z) = \frac{-n_0}{n_e} \left[\frac{4}{3\sqrt{\pi}} I_3(u_c) + \frac{\exp(-u_c^2)}{2\sqrt{\pi}} \right.$$

$$\left. \times (7 \exp(u_c^2) u_c^2 E_3(u_c^2) - 1) \right] \qquad (24)$$

$$T_e(z) = \frac{n_0}{n_e} T_0 (4 - 3 \Lambda (u_c)) \qquad (25)$$

$$q_{ze}(z) = -n_0 k T_0 \left(\frac{2kT_0}{m_e} \right)^{\frac{1}{2}} \left[- \frac{4}{3\sqrt{\pi}} I_5(u_c) \right.$$

$$\left. + \frac{7 \exp(-u_c^2)}{\sqrt{\pi}} \left(\frac{3u_c^2}{7} + \frac{27}{14} + \frac{6}{u_c^2} + \frac{12}{u_c^4} + \frac{12}{u_c^6} \right) \right] \qquad (26)$$

where ϕ is the error function; E_3 is the third exponential integral; u_c is the critical speed at which the tail is attached; and $\bar{u}_{ze}$ is the mean flow of the electron gas (which has a z-component only) normalized to the local temperature, T_0, and $I_n(x)$ is defined by,

$$I_n(x) = \int_0^x t^n \exp(-t^2) D_e(t) \, dt.$$

We note that n_e and T_e reduce to n_0 and T_0 as u_c approaches infinity. This must be the case since the distribution function then reduces to a Maxwellian plus a correction term which does not contribute to either of these moments ($f_e^{(1)} \propto \mu$). As u_c approaches infinity the mean flow and heat flux also reduce to their values predicted from collision dominated theory.

We can evaluate the effect which the tail of the distribution function has on the various moments discussed above by comparing the actual moments to the values predicted by collision dominated theory (i.e., $u_c \to \infty$). In Table 3, we list values for $\frac{n_e - n_0}{n_0}$, $\frac{T_e - T_0}{T_0}$ and $\frac{q_e - q_0}{q_0}$ as a function of temperature in the transition region. We find that the tail has very little effect on the temperature and density of the gas as predicted from collision-dominated theory. In other words, n_0 and T_0 represent the total density and mean kinetic energy of the gas to a high degree of accuracy. On the other hand, the heat flux is enhanced from that predicted by collision dominated theory by as much as thirty percent where the temperature gradient is steepest.

In the case of the mean flow for the electrons, we cannot define a quantity $\frac{\bar{u}_{ze} - \bar{u}_{zo}}{\bar{u}_{zo}}$ since, assuming that the ions and protons are effectively stationary relative to the electrons and that no net charge enters or leaves the transition region, the electric current must equal zero or $\bar{u}_{ze}$ and $\bar{u}_{zp}$ equal zero. In the presence of a temperature gradient, zero net current is maintained by a self-consistent electric field which drives cold electrons up the temperature gradient to compensate for the flow of hot electrons down the temperature gradient. We can compute the electric field, E, needed to maintain zero net current by setting equation (24) to zero. In the collison dominated case ($u_c \to \infty$), where the mean ionic charge ($\bar{Z}$) is equal to one, this electric field is given by,

$$E_0 = -0.703 \frac{k}{e} \frac{dT}{dz}$$

In Table 3, we list values for $(E - E_0)/E_0$ as a function of temperature in the transition region. We see that the tail does not affect the

value of the collision dominated electric field to any significant
degree. We also list in Table 4, values for E/E_c as a function of
temperature; we find that the self-consistent electric field is small
compared to the dynamical friction. Correspondingly, it is still a good
approximation to assume that the high energy particles streaming down
the temperature gradient do not alter their energies substantially
because of acceleration or deceleration due to an external force (See
the results of Section 4).

Because of the difficulty in determining a precise value for the
critical energy we have presented calculations for minimum and maximum
values. The results presented in Table 4 correspond to a minimum value
for the location of the tail in velocity space. In Table 4, we present
values for $\frac{q_e - q_o}{q_o}$ computed with the maximum critical energy given by
$(0.4)^{\frac{1}{2}} (u_c^2)_D$. We see that these values are all negative, meaning that
collision-dominated theory predicts a larger heat flux than the distribution
function with a tail; however, this is not physically valid since particles
cannot transport energy any faster than if they stream freely as in the
case of the high energy tail. These results indicate that if the critical
energies (used to obtain the results in Table 4) at which the tail is
attached are correct then collision-dominated theory tends to overestimate
the electron heat flux. This is not surprising since as shown in
Section 2, collision-dominated theory breaks down beyond a critical
energy plotted for the transition region in Figure 2. On the other
hand, the results obtained with the critical energy for the tail given
by $u_c^2 = (u_c^2)_E$, give heat fluxes which are greater than predicted by
collision-dominated theory. We can conclude that the actual heat flux
is quite sensitive to the location of the tail in velocity space. These
results also suggest that the critical energy for the location of the

tail cannot exceed the critical energy beyond which collision-dominated theory breaks down.[*] We note that the latter energies are closer to the

---

[*]This suggestion stems from the fact that we have incorporated the first order distribution function, $f^{(1)}$, in our total distribution function.

---

minimum critical energies used in our calculations. Indeed, as already suggested, the minimum critical energies, $(u_c^2)_E$, are probably a better estimate of the location of the high energy tails. An exact solution to this problem would require solving the Boltzmann-Fokker-Planck equation numerically - a task of enormous proportions.

6. SUMMARY

In Section 2 of this paper, we found that, based on a comparison of appropriate time scales, the electron and proton distribution functions were non-Maxwellian in the solar transition region in the sense that a high energy tail composed of hot electrons and protons streaming down from the corona would result. We also found that this anisotropy in the proton and electron distribution functions would not be reflected by the ions since their higher charge causes them to be collision-dominated and results in nearly Maxwellian distribution functions. In addition, we pointed out that the proton and electron temperatures need not be equal through the transition region and that the ions would reflect the proton temperature. If the proton temperature differs from the electron temperature in the corona then this condition would persist through the transition region. In a steady state, however, the latter condition would necessitate a source or sink of energy for one or the other species in the corona. We suggest that this would represent an interesting

line for future research since observations show line widths which are much larger than the thermal widths expected from electron temperatures derived from ionization equilibrium calculations.

In Section 3, we computed velocity space orbits for test electrons moving through a layer composed of field particles with Maxwellian distribution functions characterized by a temperature which varies through the layer. In addition, we computed the final speeds for these test electrons after they leave a layer whose depth is defined by a temperature scale height. The results were obtained from the Langevin equation which includes the effects of a dynamical friction force and an externally applied field. For the case of zero electric field, the velocity space orbits are straight lines (given by μ = constant) leading into the origin in velocity space. In computing the final energies for the test electrons, we found that an electron's energy does not change substantially over a temperature scale length for energies greater than a critical energy and that this result applies over a broad range of μ-values up to a critical value which is a function of the particle's energy. When an external electric field was included in our calculations, we found its effect was essentially to accelerate test electrons into the collisionless regime. If the electric field points along the temperature gradient, then the asymmetry produced by the temperature gradient is enhanced i.e., the number of high energy electrons moving down the temperature gradient is increased. The opposite applies if the electric field points down the temperature gradient. Furthermore, as shown by Dreicer (1960), the electric field introduces a critical surface in velocity space. If a particle's energy is less than the energy along this surface, then the dynamical friction dominates the particle's motion. If it is greater, then the particle's motion is dominated by the electric field.

The main conclusion of Section 3 was that, for a plasma with a temperature gradient, velocity space can be broken up into a thermal part, and a collisionless part populated by high energy electrons which stream through a temperature scale length without altering their energies substantially. The net result is that the electron distribution functions are characterized by high energy tails. In Section 4 we estimated the magnitude of these tails, for conditions appropriate to the transition region, and found that they were strongly over-populated relative to a Maxwellian.

In Section 5, we used the results of Section 4 to recompute various moments of the electron distribution functions. We found that the tail had a negligible effect on the total local density of electrons, the electron temperature, or on the critical self-consistent electric field needed to maintain zero net current. On the other hand, the effect of the high energy tail is to enhance the electron heat flux over that computed from collision-dominated theory by a maximum of 30% in the temperature range from $10^{5.2}$ - $10^{5.4}$ K. We also found, however, that these results are sensitive to the location of the high energy tail in velocity space and that detailed calculations, which would involve solving the Boltzmann-Fokker-Planck equation numerically, are necessary in order to determine the exact magnitude of these effects. Nevertheless, we feel that the minimum critical energies represent a good approximation for the locations of the tails and that the results obtained with these critical energies are reasonable approximations for the enhancement in heat flux.

The enhancement in the heat flux, which we computed for Dupree's model will not have a serious effect on the energy budget of the corona and the transition region. However, it is important to realize that the computed enhancement is sensitive to the location of the critical energy.

Indeed, the increase in heat flux relative to that computed from collision-dominated theory may be significant for regions which have lower densities and/or larger temperature gradients (i.e., lower critical energies) than obtained from Dupree's model. A similar analysis for coronal holes and active regions, for example, may yield interesting results.'

ACKNOWLEDGEMENTS

REFERENCES

Chapman, S. and Cowling, T. G.: 1970, The Mathematical Theory of

   Non-Uniform Gases, 3rd edition, Cambridge University Press.

Dreicer, H.: 1959, Phys. Rev. 115, 238.

Dreicer, H.: 1960, Phys. Rev. 117, 329.

Dupree, A. K.: 1972, Astrophys. J. 178, 527.

Roussel-Dupré, R. A.: 1979, University of Colorado, Ph.D. thesis (unpublished).

Spitzer, L. and Härm, R.: 1953, Phys. Rev. 89, 997.

Spitzer, L.: 1962, Physics of Fully Ionized Gases, 2nd edition, No. 3,

   Interscience Publications.

Table I

Fraction f of Particles with Energy Above u^2

in a Maxwellian Distribution

u^2	$1 - f$	f
1.00(-4)	7.52(-7)	1.00
1.00(-2)	7.48(-4)	1.00
1.00(-1)	2.32(-2)	9.77(-1)
5.00(-1)	2.01(-1)	7.99(-1)
1.00	4.28(-1)	5.72(-1)
2.00	7.36(-1)	2.64(-1)
4.00	9.54(-1)	4.60(-2)
6.00	9.93(-1)	6.85(-3)
8.00	9.99(-1)	1.07(-3)
1.00(1)	1.00	1.62(-4)
5.00(1)	1.00	1.54(-21)
1.00(2)	1.00	4.20(-43)

Table II

The Dynamical Friction Force for Electrons

u	F_{D/eE_c}
0.0	0.00
1.0 (-4)	5.90
1.0 (-2)	5.36 (2)
2.0 (-2)	7.83 (2)
2.3 (-2)	7.84 (2)
3.0 (-2)	7.37 (2)
1.0 (-1)	1.00 (2)
2.0 (-1)	2.53 (1)
3.0 (-1)	1.15 (1)
5.0 (-1)	4.65
1.0	1.86
1.4	1.26
1.8	8.70 (-1)
2.0	7.27 (-1)
2.5	4.80 (-1)
3.0	3.33 (-1)
4.0	1.88 (-1)
5.0	1.20 (-1)

Table III

Moments of the Electron Distribution Functions[*]

Log T	$\dfrac{n - n_0}{n_0}$	$\dfrac{T - T_0}{T_0}$	$\dfrac{q_e - q_0}{q_0}$	$\dfrac{E - E_0}{E_0}$	$\dfrac{E}{E_c}$
4.7	7.56(-11)	4.4(-9)	-1.00(-5)	2.03(-6)	1.31(-4)
4.8	1.88(-6)	7.2(-5)	-5.11(-3)	-1.52(-3)	7.89(-4)
5.0	4.09(-4)	1.2(-2)	1.21(-1)	1.20(-2)	4.82(-3)
5.2	1.94(-3)	5.1(-2)	2.83(-1)	3.50(-3)	1.12(-2)
5.4	1.31(-3)	3.6(-2)	2.92(-1)	1.38(-2)	8.87(-3)
5.6	7.37(-4)	2.1(-2)	1.69(-1)	1.44(-2)	6.52(-3)
5.8	4.09(-4)	1.2(-2)	8.59(-2)	5.98(-4)	5.02(-3)
6.0	2.05(-4)	6.2(-3)	4.73(-2)	-2.29(-3)	3.66(-3)
6.2	1.13(-4)	3.5(-3)	1.89(-2)	3.32(-3)	2.87(-3)

[*]The subscript (o) refers to moments computed from collision dominated theory. Those without the subscript are computed with the effect of the tail included.

Table IV

Comparison of Electron Heat Flux Calculations[*]

Log T	u_{zc}^2	$\dfrac{q_e - q_0}{q_0}$
4.7	66	0
4.8	27	-7.70(-7)
5.0	11	-3.45(-2)
5.2	7.0	-1.80(-1)
5.4	8.2	-1.02(-1)
5.6	9.5	-7.04(-2)
5.8	11	-3.51(-2)
6.0	13	-1.41(-2)
6.2	14	-5.45(-3)

[*] q_e is the heat flux computed with the effect of the of the tail included while q_0 is the collision dominated value.

FIGURE CAPTIONS

Figure 1   Ratio of electron mean free path to temperature scale length for thermal electrons in the Solar Transition Region.

Figure 2   Critical energies at which the first order electron distribution function equals the Maxwellian.

Figure 3   Critical energies at which the first order proton distribution function equals the Maxwellian.

Figure 4   Critical energies for 90° deflection and thermalization of electrons.

Figure 5   Critical energies for a 90° deflection and theramalization of protons.

Figure 6   Critical energies for a 90° deflection and thermalization of Si IV.

Figure 7   Final velocities for test electrons injected into a given layer in the transition region for two initial energies.

Figures 8-11   Final velocities for test electrons injected into a given layer in the transition region with an electric field.

Figure 12   Ratio of the electron high energy tail to a Maxwellian.
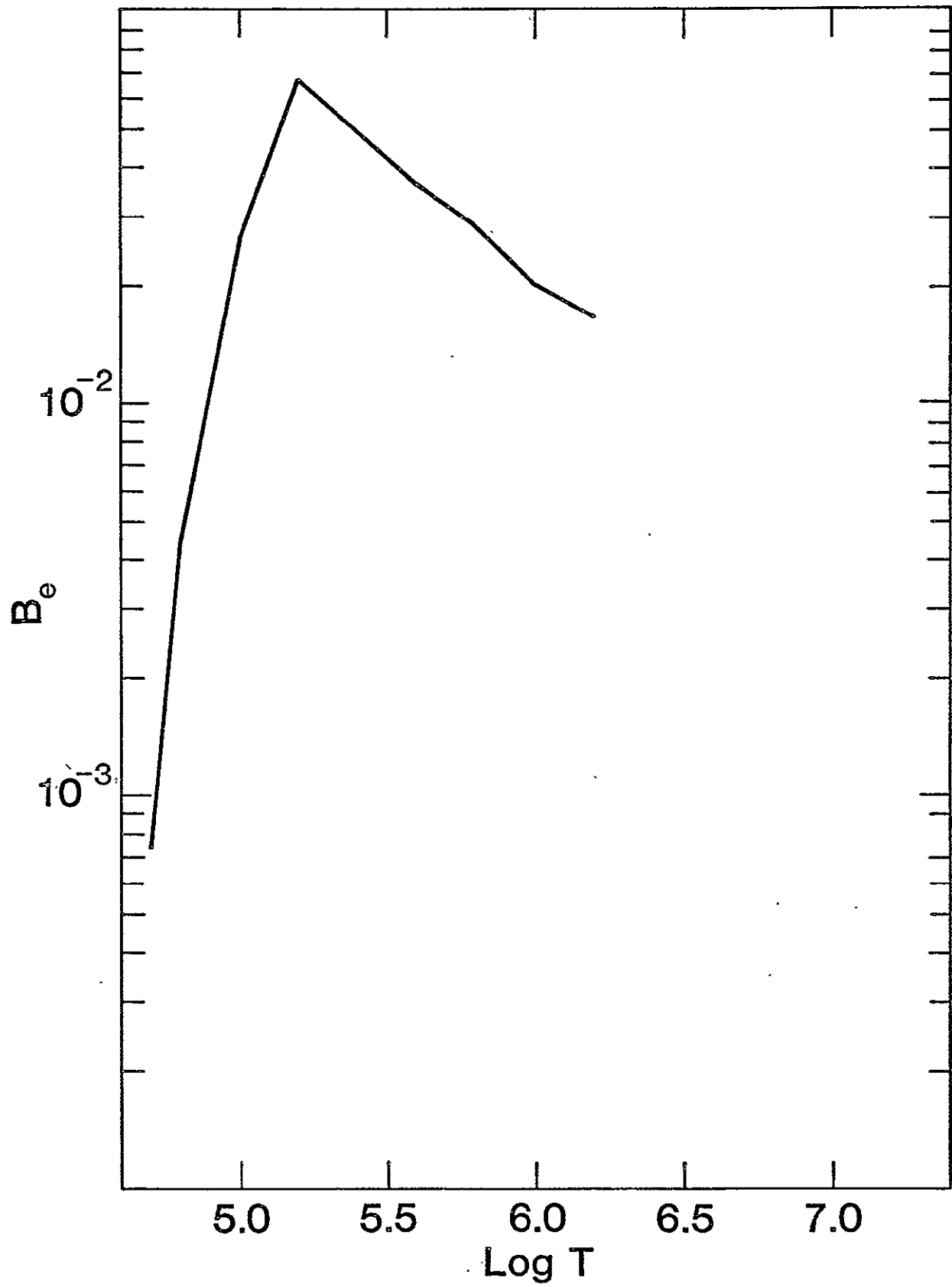
Figure 1
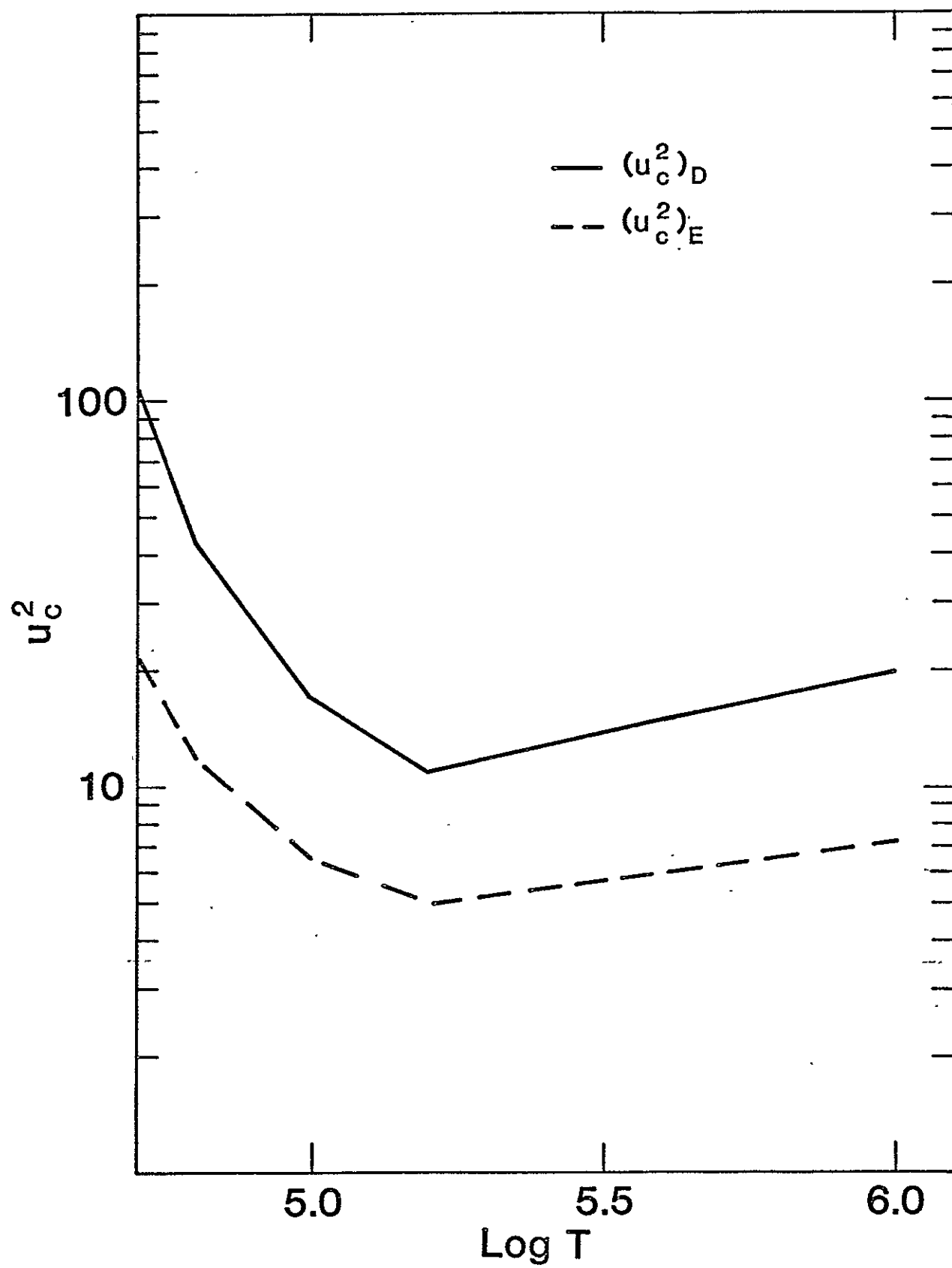
Figure 4
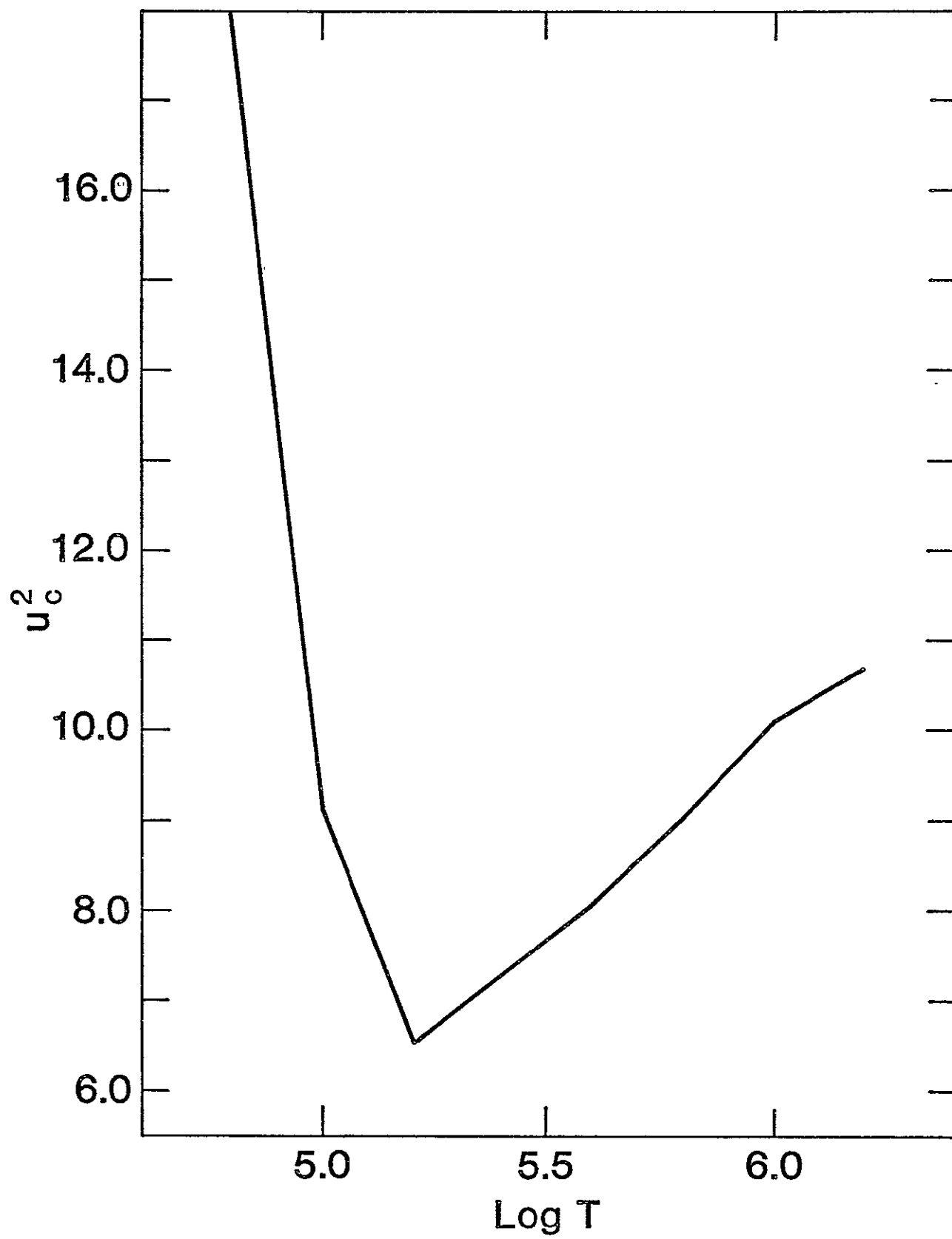
Figure 3
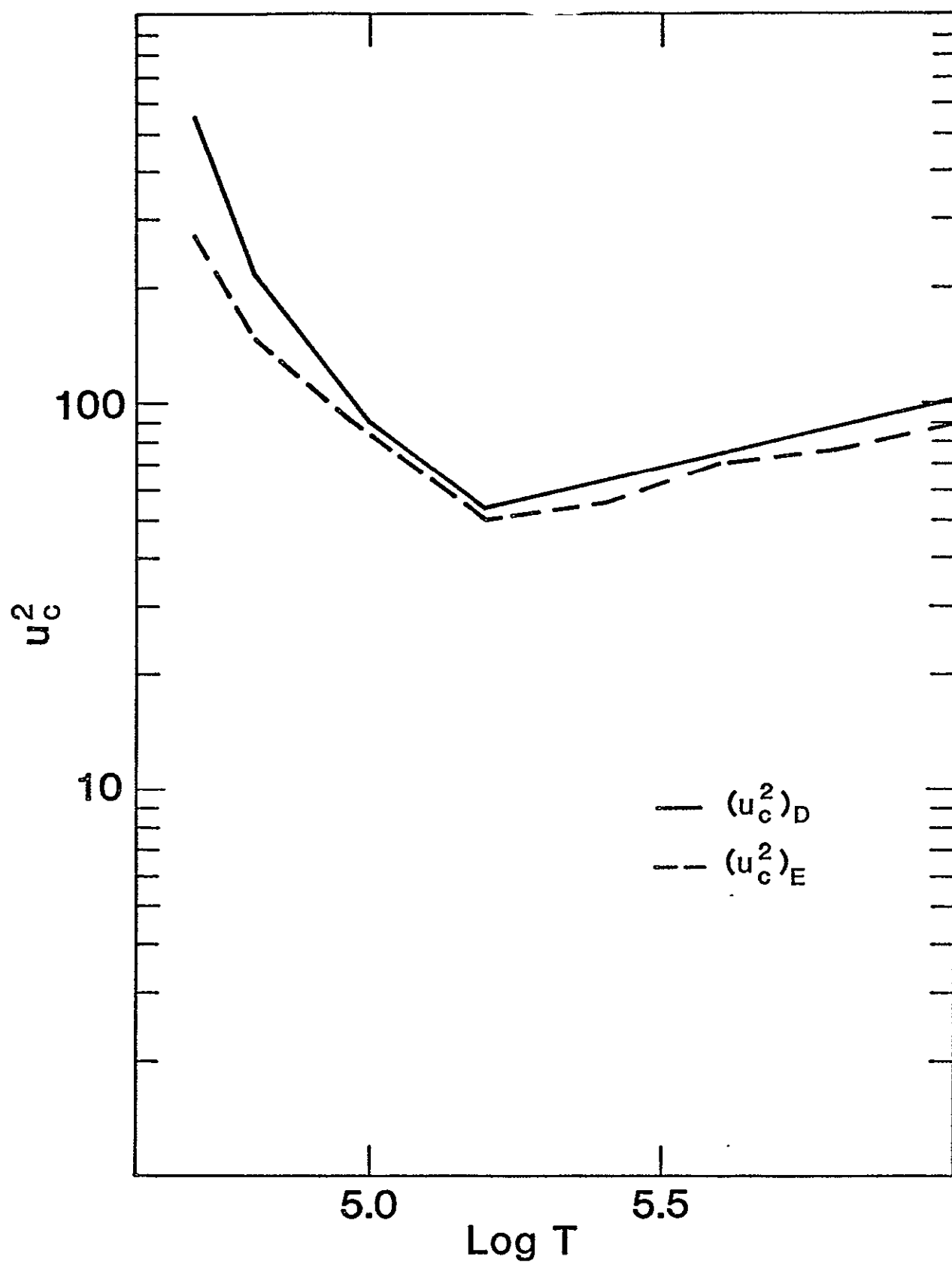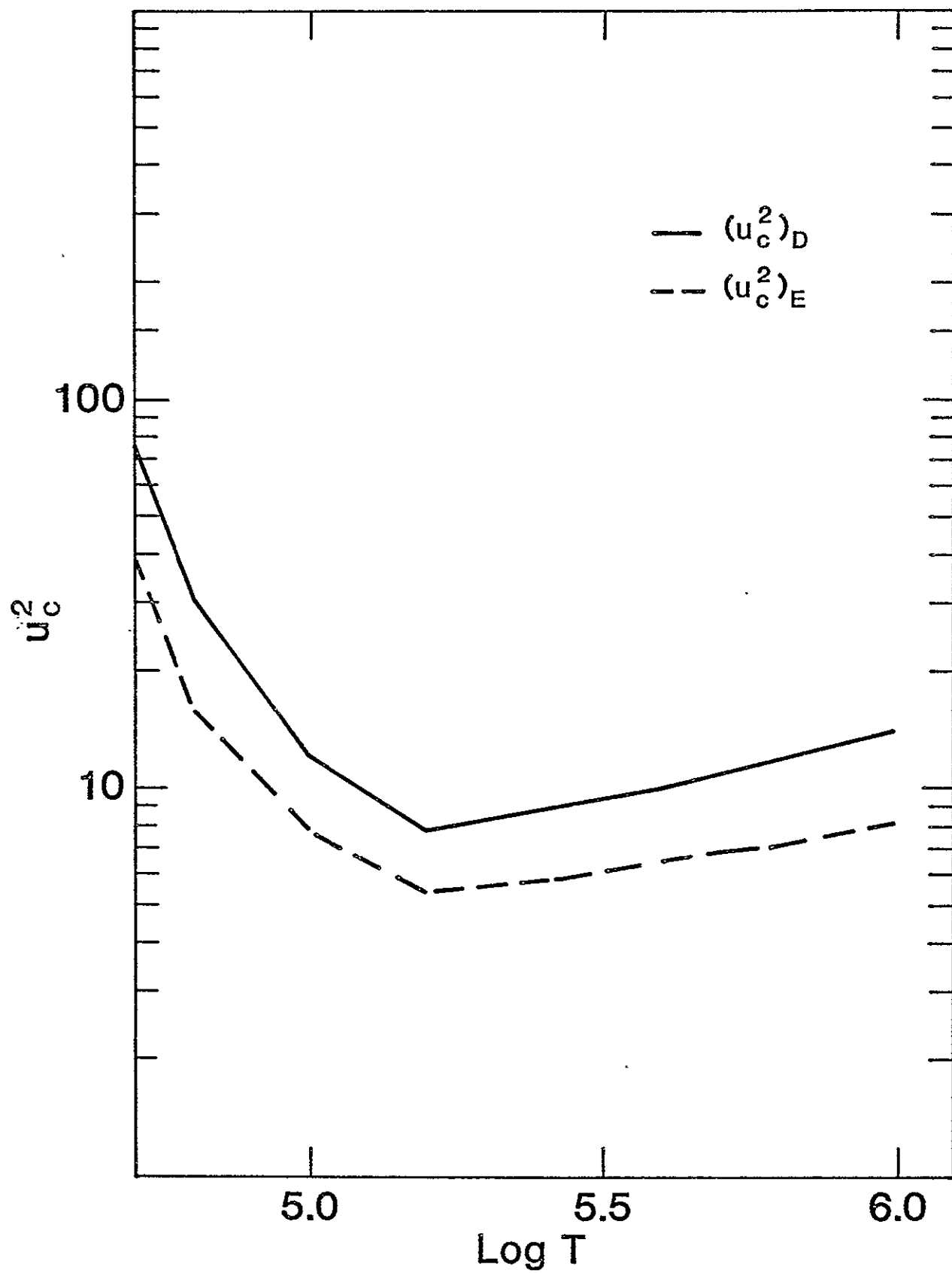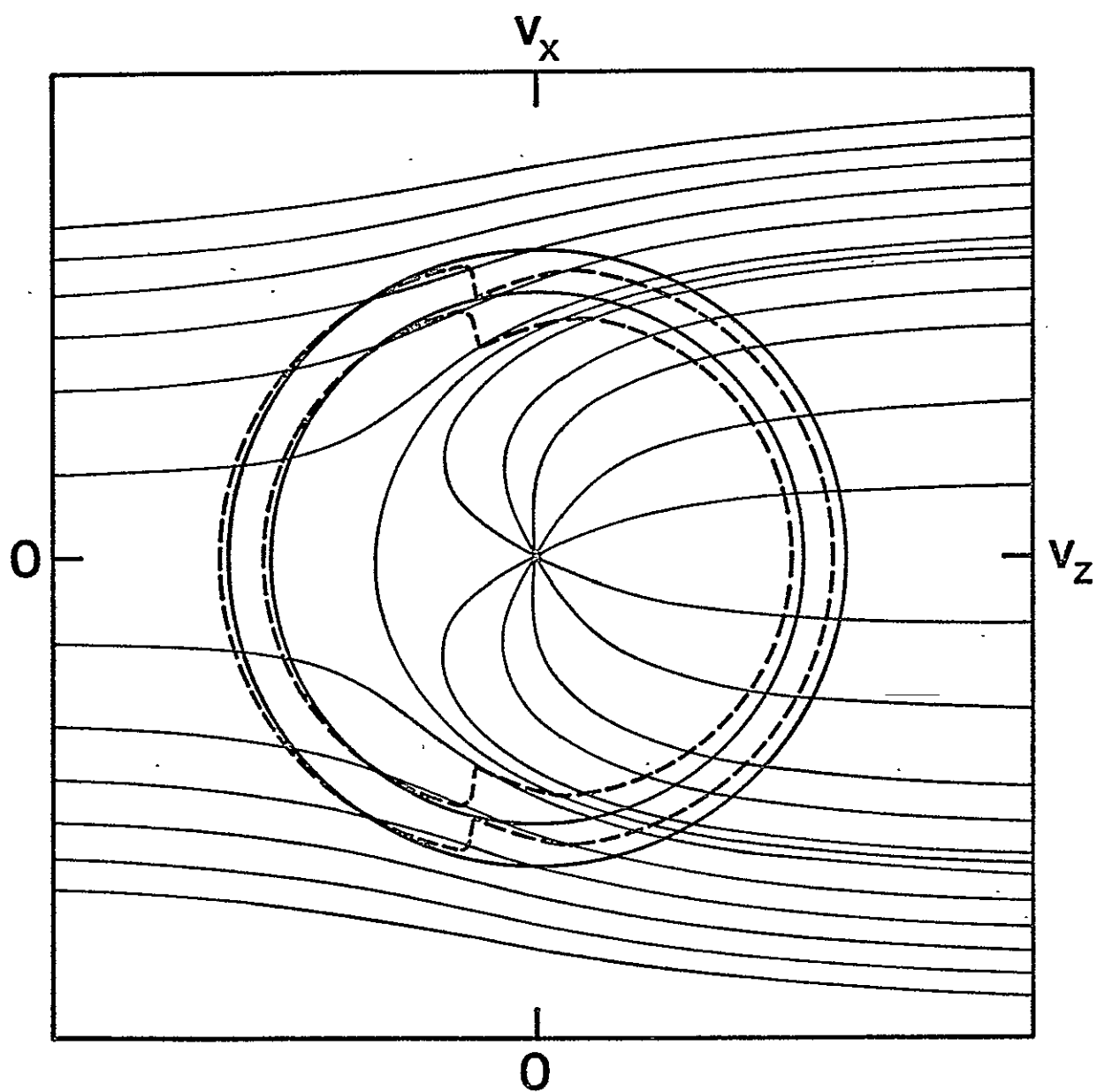
Figure 6

Figure 5

$$u_c^2 = 11, \beta = 0.5$$

Figure 8
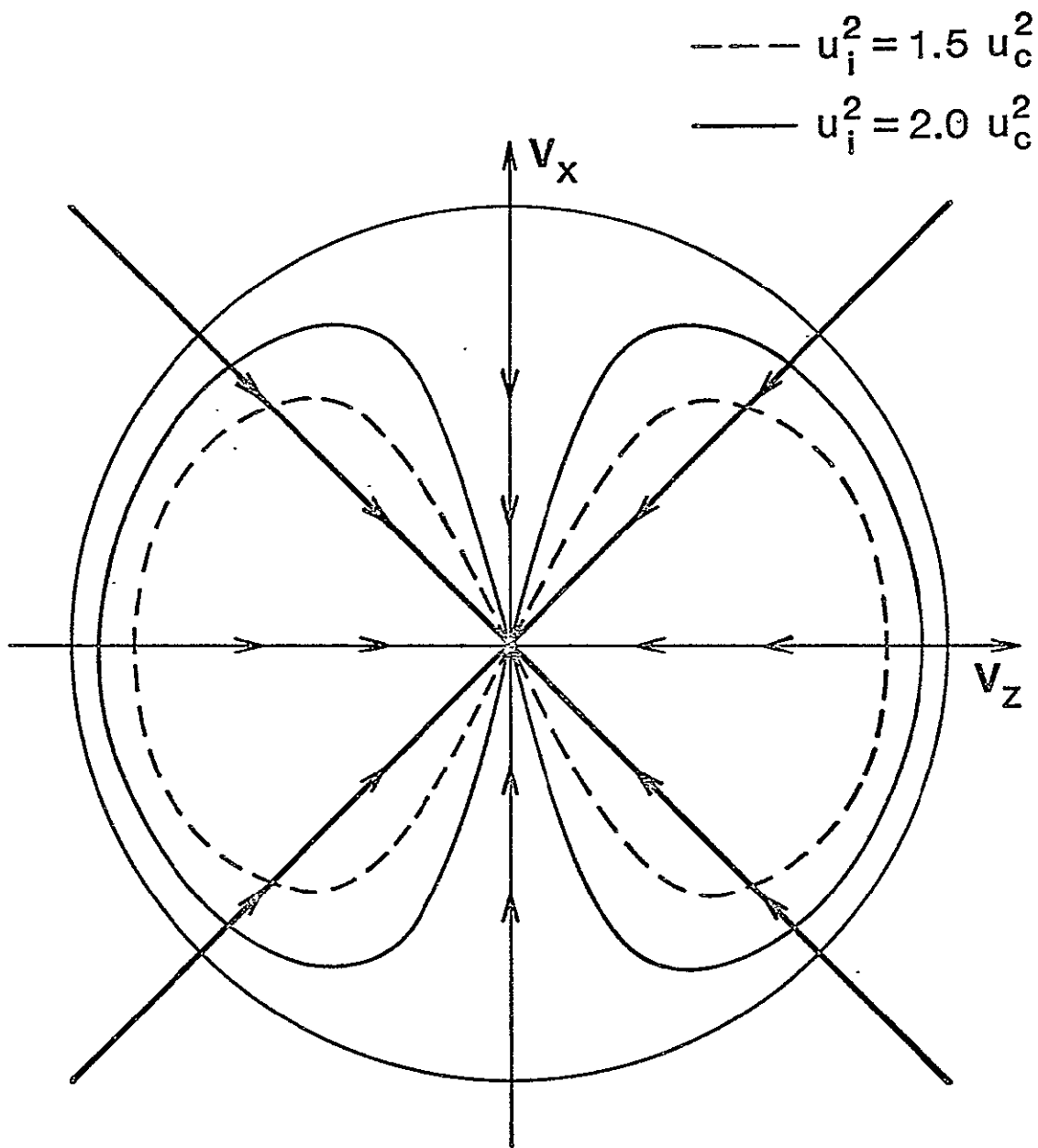
Figure 7
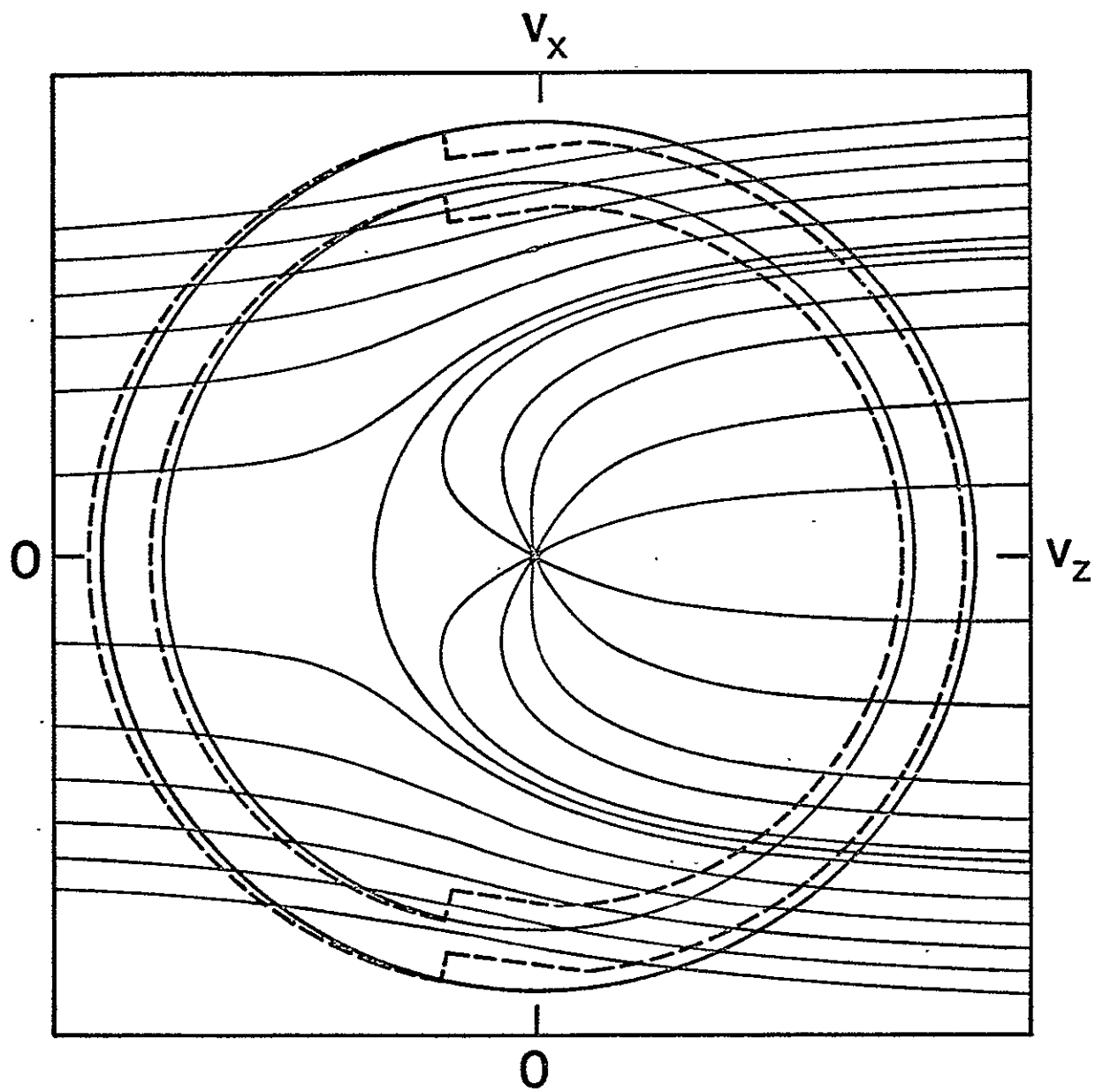
Figure 10

Figure 12

V_X

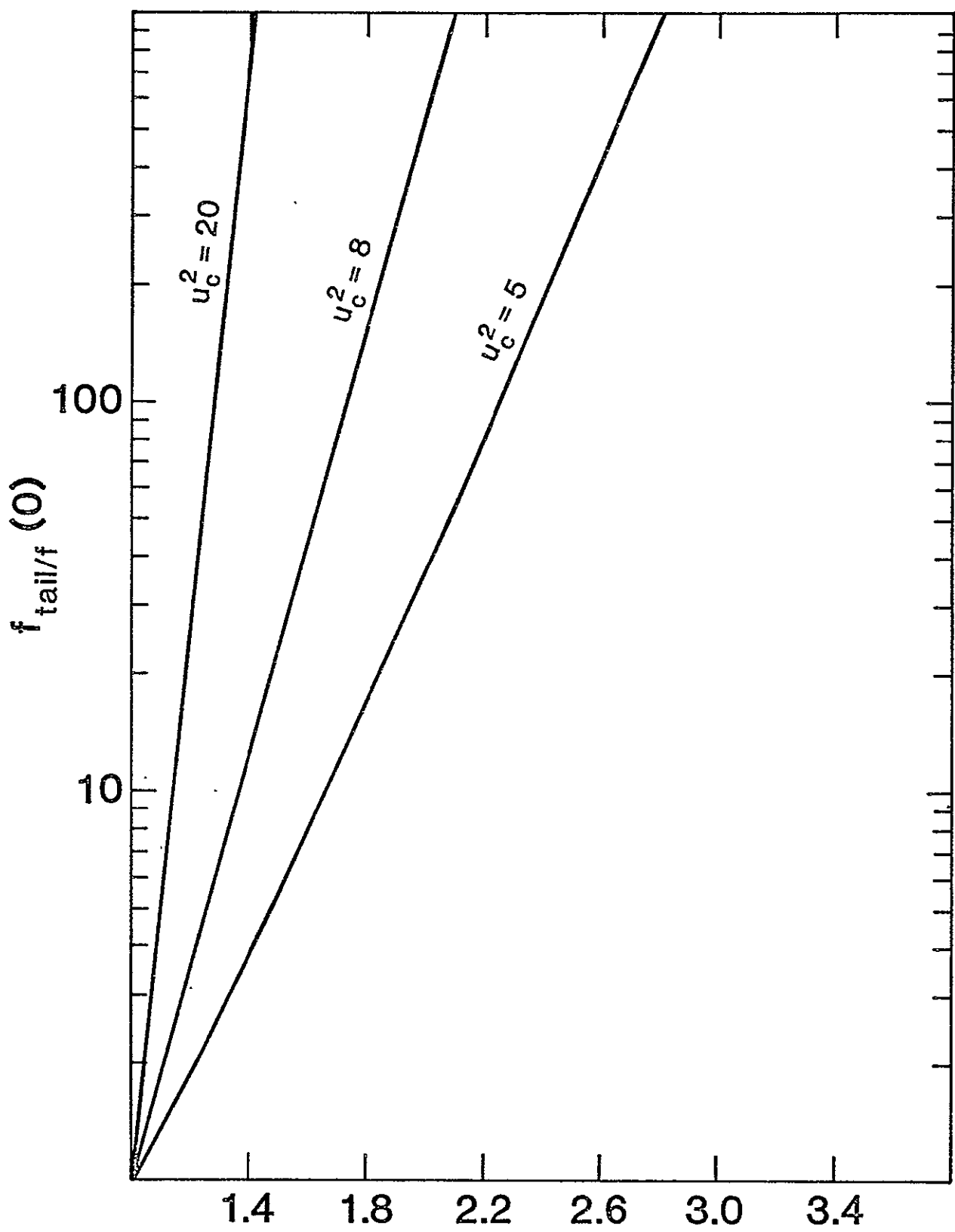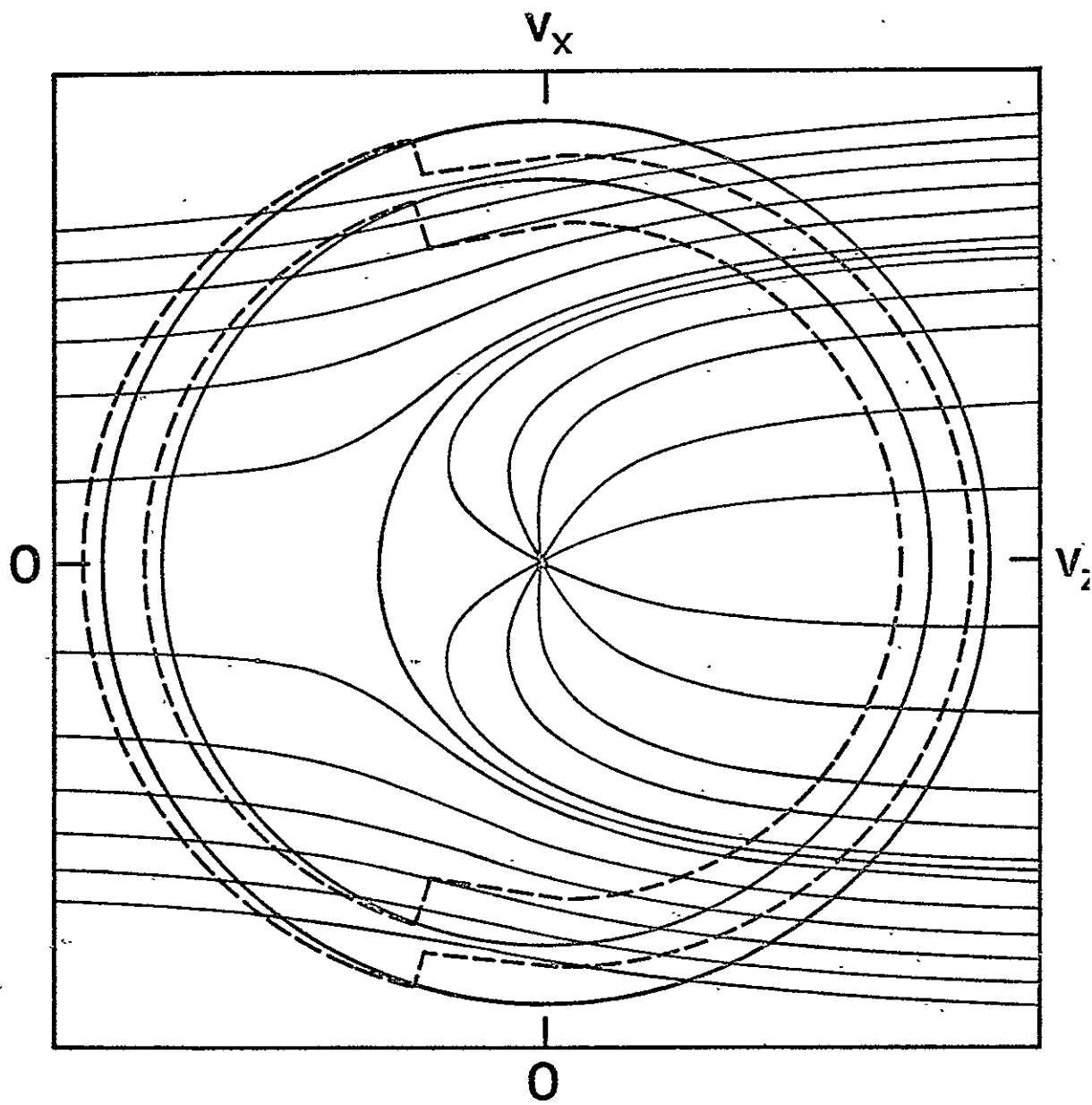O V_2

O

$$u_c^2 = 11, \beta = 1.0$$

Figure 9

APPENDIX I

DERIVATION OF THE WORK DONE ON A FAST ELECTRON OVER
A TEMPERATURE SCALE LENGTH

The dynamical friction force which appears in the Langevin equation includes the effect of deflections in slowing a beam of particles. The deflections, however, do not remove energy from the beam but simply redirect some of that energy into the perpendicular direction. For our purposes, we are interested in computing the amount of energy lost by a fast electron to the field particles during Coulomb encounters over a temperature scale length. More precisely, given a test electron's initial energy, we wish to compute its final energy after it travels a temperature scale length.

The change in energy experienced by a test particle during a single encounter can be written as,

$$\Delta E = \frac{1}{2} m_e \left(\Delta v_{\perp}^2 + \Delta v_{//}^2 + 2v \ \Delta v_{//}\right) \qquad \text{(I-1)}$$

where perpendicular and parallel here are taken relative to the initial direction of motion. Averaging (I-1) over all impact parameters and field particle velocities, assuming a Maxwellian distribution function for the field particles, we obtain a general expression for the average rate of energy exchange with the field particles (See Spitzer 1962),

$$\frac{<\Delta E>}{kT} = 2n_t \Gamma_t a_t^{3/2} \sum_f \frac{n_f z_f^2}{n_t z_t^2} \ \frac{1}{u} \left(\phi \ (\beta_f u) \right.$$

$$\left. - (1 + \beta_f^{-2}) \Lambda \ (\beta_f u) \right) \qquad \text{(I-2)}$$

In the absence of any external forces, the rate of energy loss for a
fast electron moving through an electron-proton gas is obtained from
equation (I-2) and is given by,

$$\frac{d\,\dfrac{u^2}{a_e}}{dt} = -\frac{2n_e \Gamma_e\, a_e^{\frac{1}{2}}}{u} \qquad (I\text{-}3)$$

where we have assumed that $n_e = n_p$. The time, t, in the above equation
is taken along a particle trajectory and is related to the z-coordinate
in our layer by,

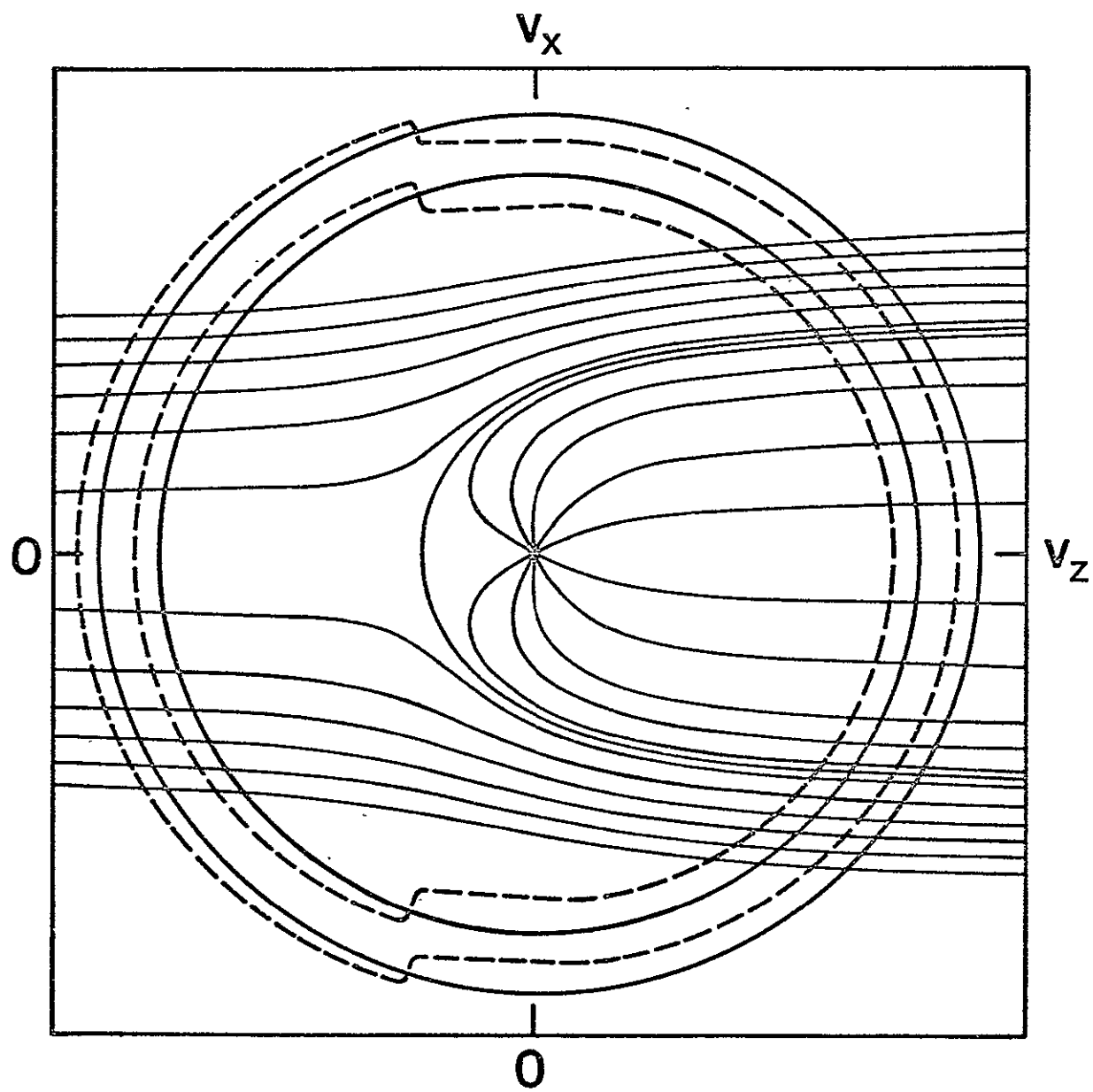$$\frac{dz}{dt} = \mu v. \qquad (I\text{-}4)$$

We can now make a change of variables where the temperature along a
particle's trajectory replaces the time in equation (I-3). Assuming
that the field particle densities and the temperature gradient are
constant, we have,

$$\frac{d(u^2\theta)^2}{d\theta} = -\frac{4n_e \Gamma_e a_0^2}{\mu}\left(\frac{1}{T_0}\frac{dT}{dz}\right)^{-1} \qquad (I\text{-}5)$$

where $\theta = T/T_0$ and $a_0 = \dfrac{m_e}{2kT_0}$

The solution to (I-5) is simply,

$$u_f^4 = u_0^4 - \frac{4n_e \Gamma_e a_0^2}{\mu}\left(\frac{1}{T_0}\frac{dT}{dz}\right)^{-1}(\theta_0 - \theta_f) \qquad (I\text{-}6)$$

v_x

0

v_z

0

$u_c^2 = 22, \beta = 1.0$

Figure 11

where u_f is the final speed normalized to the thermal speed at

T_o and u_o is the initial particle speeds. Given that,

$$4n_e \Gamma_e a_o^2 \left(\frac{1}{T_o} \frac{dT}{dz}\right)^{-1} = 2\delta_c,$$ equation (I-6) reduces to the desired

result - equation (14).